ELSEVIER

Biophysical Chemistry 57 (1996) 143–153

Biophysical Chemistry

Simulation of state 4 → state 3 transition in isolated mitochondria

Bernard Korzeniewski

Institute of Molecular Biology, Jagiellonian University, al. Mickiewicza 3, 31-120 Kraków, Poland

Received 16 July 1994; revised 22 March 1995; accepted 23 May 1995

Abstract

The mathematical dynamic model of oxidative phosphorylation developed previously and in the accompanying paper was modified to involve isolated mitochondria conditions; it was also used to simulate state 4 → state 3 transition in rat liver mitochondria incubated with succinate as respiratory substrate and glucose–hexokinase as an ADP-regenerating system. Changes in the respiration rate, protonmotive force and reduction level of ubiquinone and cytochrome *c* as well as the internal (i) and external (e) ATP/ADP ratio between state 4 and state 3 were calculated and compared with the experimental data. Flux control coefficients with respect to oxygen consumption flux for different reactions and processes of oxidative phosphorylation were simulated for different values of the respiration rate (state 4, state 3 and intermediate states). Flux control coefficients for the oxidation, phosphorylation and proton leak subsystems with respect to the oxidation, phosphorylation and proton leak fluxes for different values of the respiration rate were also calculated. These theoretical data were compared with the experimental results obtained in the frame of metabolic control analysis and the 'top-down' approach to this analysis. A good agreement was obtained. Simulated time courses of the respiration rate, the protonmotive force (Δp) and other parameters after addition of a small amount of ADP to mitochondria in state 4 mimicked at least semiquantitatively the experimentally measured time courses of these parameters. It was concluded, therefore, that in the present stage, the model is able to reflect different properties of the oxidative phosphorylation system in a broad range of conditions fairly well, allows deeper insight into the mechanisms responsible for control and regulation of this process, and can be used for simulation of new experiments, thus inspiring experimental verification of the theoretical predictions.

Keywords: Oxidative phosphorylation; Dynamic model; Computer simulation; Metabolic control analysis; Metabolic regulation

1. Introduction

State 3 of isolated mitochondria was defined [1] as a state with external ADP added and a high respiration rate. When all ADP is converted to ATP, mitochondria transfer to state 4, with low respiration rate. In state 3, there is an intensive phosphorylation flux (ATP synthesis) and a relatively low protonmotive force. In state 4 the phosphorylation flux vanishes completely and the respiration rate corresponds entirely to the proton leak; the protonmotive force is high. State 3 can be also generated from state 4 by addition (in excess) of an ADP-regenerating system, for example glucose + hexokinase. If such a system is added in sub-saturating amounts, intermediate states between state 4 and state 3 are reached. State 3 obtained with an ADP-regenerating system is more physiological that state 3 induced by addition of ADP: the ADP-regenerating system mimics an ATP-utilising system present in intact cells.

SSDI 0301-4622(95)00076-3

State 4 → state 3 transition is a simple and very broadly analysed model for regulation of respiration and ATP synthesis in intact cells.

The mechanisms responsible for control and regulation of oxidative phosphorylation in mammalian mitochondria are currently quite well known [2–4]. Changes in many parameter values have been measured (e.g. respiration rate, Δp, internal and external ATP/ADP, NADH/NAD$^+$) during state 4 → state 3 transition [5–13] and their qualitative role in regulation has been determined. The results obtained were somewhat different depending on the kind of mitochondria as well as the isolation procedure, incubation medium and respiratory substrate used. The flux control coefficients for different parts of oxidative phosphorylation with respect to oxidation flux (respiration rate) have been measured [7,8] as well as the flux control coefficients for the oxidation, phosphorylation and proton leak subsystems with respect to the oxidation, phosphorylation and proton leak fluxes for different values of the respiration rate [5]. However, all these data concern the macroscopic level. To understand the control and regulation of the oxidative phosphorylation process more deeply it is necessary to derive macroscopic properties of the system from microscopic characteristics of its components in a quantitative way. Because of the great complexity of the system, mathematical models are necessary.

Several different kinds of description have been applied to oxidative phosphorylation. Metabolic control analysis (MCA) [14–16] proved to be a very useful tool for studying control and regulation of oxidative phosphorylation in a quantitative way. However, this method is only a phenomenological description, unable to provide a deeper explanation. Furthermore, it concerns only the steady state properties and not changes in time. Non-equilibrium thermodynamics [17,18] and mosaic non-equilibrium thermodynamics [18,19] allow to deal with many different aspects of oxidative phosphorylation, especially those concerning energetic and thermodynamic aspects of this process. Nevertheless, these approaches are also rather phenomenological and use terminology not very familiar for many biochemists. In principle, the most complete description of any metabolic pathway would be a full mechanistic kinetic description, expressing the behaviour of the pathway in terms of metabolite concentrations, enzyme kinetics, pool sizes, buffering capacities and other similar parameters. Moreover, it would be possible to derive the properties described by other approaches from a correct kinetic description, and to explain all phenomena occurring at physiological level using this description.

However, a full mechanistic description of oxidative phosphorylation is not possible now because of the great complexity of the system and limitations of our knowledge. This statement concerns particularly kinetic properties of particular enzymes and processes. Nevertheless, it is possible to develop a quasi-mechanistic approach, where some reactions are grouped into blocks (for example substrate dehydrogenation) and described by simplified kinetic expressions. Such a quasi-mechanistic description would retain most advantages of a full mechanistic description. However, because of simplifications and assumptions made, it would have to be tested in a broad range of different conditions.

Two quasi-mechanistic kinetic models of oxidative phosphorylation have already been applied to simulate the state 4 → state 3 transition [20–22]. However, both models mentioned have some disadvantages. The model developed by Holzhütter et al. [20] assumes three enigmatic proton pumps before cytochrome *c* and linear dependence of proton leak on Δp; equations B and D in Table 1 in [20] are incorrect (both should contain the factor $\delta + 1$ in a power expression); the size of the internal adenine nucleotide pool was understated to obtain time courses of parameters consistent with experiments. The model developed by Bohnensack [21] (very important as the first model of this kind) is a static one, it operates on oversimplified descriptions of cytochrome oxidase and proton leak, uses an outdated model of the ATP/ADP carrier, does not take into account magnesium complexes of adenine nucleotides and involves an enigmatic external ATPase, which is necessary to obtain correct theoretical predictions. Additionally, experimental verification of both models is rather limited. A more recent model of oxidative phosphorylation developed by Korzeniewski and Froncisz [17,18] describes only an intermediate state $3_{1/2}$ in isolated mitochondria.

The purpose of the present work is to extend this model and simulate the properties of the oxidative

phosphorylation system studied in four kinds of experiments (and therefore to perform a broad testing of the model):

(1) measurements of changes of different parameter values (i.e. respiration rate, Δp, internal and external ATP/ADP, UQ/UQH_2; UQ being the oxidised form of ubiquinone and UQH_2 the reduced form of ubiquinone) during state 4 → state 3 transition induced by an addition of excess of hexokinase,

(2) measurements of flux control coefficients for different enzymes (processes) of oxidative phosphorylation with respect to the respiration flux for different values of the respiration rate in the frame of metabolic control analysis [7,8,14–16],

(3) measurement of flux control coefficients for the oxidation, phosphorylation and proton leak subsystems with respect to the oxidation, phosphorylation and proton leak fluxes for different values of the respiration rate in the frame of the 'top-down' approach to metabolic control analysis [5,25],

(4) time courses of the respiration rate, Δp, UQ/UQH_2, external adenine nucleotide concentrations and other parameters after addition of a small amount of ADP to mitochondria in state 4 (transfer to state 3 and, after exhaustion of ADP, return to state 4).

The model, when successfully tested, should be able to describe the control and regulation of oxidative phosphorylation in 'typical' (i.e. from liver or muscle, but not from brown adipose tissue) mammalian mitochondria correctly. Since the majority of the data used for model building were obtained for rat liver mitochondria with succinate as respiratory substrate, the quantitative predictions of the model concerns especially this kind of mitochondria and substrate.

2. Model

The modified model of oxidative phosphorylation presented in the accompanying paper was adjusted to isolated mitochondria conditions as described in [23,24]. Comparing with the model for the cell, the following changes are introduced:

(1) lack of cell volume – concentrations of external ATP, ADP, AMP and P_i are determined in a suspension volume;

(2) the external concentration of inorganic phosphate is 10 mM and of the adenine nucleotide pool is 1 mM, in agreement with experimental conditions [7,8]; concentrations of particular nucleotides were adjusted to obtain the external and internal phosphorylation potentials in the 'physiological' state $3_{1/2}$ comparable with those on intact cells, maintaining the same displacement from equilibrium of the ATP/ADP carrier and phosphate carrier;

(3) only two coupling sites are considered (complex III and IV), since succinate is used as substrate; the respiration rate is increased 1.7 times to maintain the phosphorylation rate at the same level;

(4) the external ATP consumption is described as [ATP]-dependent, with Michaelis–Menten constant equal to 150 μM, what reflects the kinetic properties of hexokinase;

(5) a different description for the substrate dehydrogenation was used; this is justified, since substrate dehydrogenation in isolated mitochondria with succinate as substrate is quite different from substrate dehydrogenation in intact cells.

The details of the changes mentioned above and some additional changes are named below.

The substrate dehydrogenation system (for succinate as substrate) contains two components: dicarboxylate carrier and succinate dehydrogenase. The kinetics of this system was described by the following simple phenomenological equation:

$$\nu_{DEHU} = k_{DEHY}(U_0 - UQH_2) \quad (1)$$

where U_0 is equal to $0.7 \cdot U_t$. This equation was chosen to obtain a linear dependence of the oxidation flux on Δp (all other kinetics tested did not fulfil this requirement). Substrate concentration was not taken into account explicitly, since it was assumed to be constant (external succinate in excess). Because $[UQH_2]$ and [UQ] are related to each other by the following relationship: $[UQH_2] + [UQ] = \text{const}$, the above phenomenological dependence on $[UQH_2]$ contains implicitly also a dependence on [UQ].

The applied expression for flux intensity through the respiratory chain (complex III in this case, since cytochrome oxidase was described separately) was:

$$\upsilon_{CHAIN} = k_{CHAIN} \cdot \Delta G_{CHAIN} \quad (2)$$

where $\Delta G_{chain} = \Delta E_{chain} - \Delta p \cdot (4 - 2u)/2$. The parameter u was constant and equal to $\Delta\Psi/\Delta p$ and

the term $(4-2u)/2$ reflected the numbers of protons and changes transported by complex III (these numbers are not equal for this complex – it transports 4 protons, but only 2 charges). The value of the mid-point redox potential of the ubiquinone pool (including complex III) was equal to 85 mV [26].

The dependence of proton leak on Δp obtained experimentally in [5] can be approximated fairly well for Δp values greater than 160 mV by the following equation:

$$\nu_{LEAK} = k_{LEAK}(\Delta p - \Delta p_0) \quad (3)$$

where $\Delta p_0 = 160$ mV. However, calculations using the dependence described in the previous paper [23] gave quite similar results. Therefore, a particular kinetic description of proton leak did not influence the obtained results significantly.

The respiratory chain, ATP synthase and phosphate carrier were described as working near equilibrium (all three reactions were displaced from equilibrium 1.1 times in state $3_{1/2}$), although this assumption is probably fulfilled only approximately. When greater (even 100 times) displacement of the respiratory chain from equilibrium was introduced, it did not change the results significantly.

State 3 and intermediate states were obtained from state 4 by an introduction of different values of ATP utilisation activity (what corresponds to different concentrations of hexokinase).

The numerical procedures used were the same as in the accompanying paper.

3. Theoretical results and discussion

Simulated changes in values of chosen parameters during state 4 → state 3 transition are presented in Table 1. The comparison with experimental results can be often only semiquantitative, as these results differ somewhat depending on the source of mitochondria, isolation procedures, incubation medium and respiratory substrate added. Taking this limitation into consideration, a good agreement between experimental [5–13] and simulated absolute values of parameters and their changes can be stated. For example, the calculated about 5-fold increase in the respiration rate is a typical value measured experimentally for mitochondria incubated with succinate [5,7–9,12,13]. The obtained decrease in the protonmotive force by about 20 mV is at the lower limit of a broadly accepted range of 20–30 mV [5,9,12,13]; even lower changes in Δp during state 4 → state 3 were measured experimentally [12]. The 10 times lower internal ATP/ADP ratio obtained as a result of simulations in state 3 as compared to state 4, is comparable with an about 8-fold decrease of this ratio in state 3 obtained in [6]. Theoretical values of other parameters (and their changes) in state 4, state 3 and intermediate states are also consistent, at least roughly, with experimental measurements [6,9,10]. This suggests that the model describes at least the general steady-state properties of isolated mitochondria well.

Some conclusions concerning regulation of particular enzymes (processes) of oxidative phosphorylation during state 4 → state 3 transition can be drawn from the theoretical results mentioned above. Cytochrome oxidase seems to be activated mainly by a decrease in Δp, rather than an increase in a reduction level of cytochrome c (this increase is very small). The opposite situation occurs during the aerobiosis → anaerobiosis transition [23], where the cytochrome c reduction level is at least as important as a regulatory factor as the protonmotive force; reduc-

Table 1
Simulated values of chosen parameters in state 4, state $3_{1/2}$ (about 50% of state 3 respiration rate) and state 3

Parameter	State 4	State $3_{1/2}$	State 3	Change
Respiration rate (nmol O_2/min/mg protein)	20	57	101	↑5.05 times
Δp (mV)	185.9	175.0	166.0	↓19.9 mV
UQ/UQH_2	0.58	1.09	2.43	↑4.19 times
$cyt.c^{3+}/cyt.c^{2+}$	4.88	4.17	4.23	↓1.15 times
ATP_i/ADP_i	10.5	2.73	1.00	↓10.5 times
ATP_c/ADP_c	7054	24.0	0.62	↓11377 times

tion of cytochrome c seems thus to be tightly linked with oxygen tension. In the respiratory chain the decrease in Δp overcomes an oxidation of UQ pool, which, on the other hand, activates the substrate dehydrogenation process. The respiratory chain, ATP synthase and phosphate carrier work near equilibrium and a small displacement from equilibrium can activate them to a required extent [27]. In the case of the ATP/ADP carrier a great fall in the external ATP/ADP ratio overcomes a decrease in the internal ATP/ADP ratio and Δp ($\Delta\Psi$). The simulated external ATP/ADP ratio in state 4 is very high since no external ATPase activity is taken into account; mitochondrial preparations are frequently contaminated with some external ATPases and therefore this ratio under experimental conditions is somewhat lower. An addition of a small external ATP usage in the model allows to decrease the external ATP/ADP ratio in state 4 to the appropriate value. The ATP-utilising system (hexokinase) is regulated by external ATP at concentrations below the Michaelis–Menten constant for this compound (150 μM) and is insensitive to ATP at concentrations significantly exceeding this constant.

Table 2 and Fig. 1 show simulated values of flux control coefficients for particular enzymes (reactions) of oxidative phosphorylation with respect to the oxidation flux for different values of the respiration rate. The obtained pattern of control is similar to the experimental results obtained by Groen et al. ([8], Table 1 and Fig. 3) and Gellerich et al. [7] (somewhat more similar to the results from the latter paper). The ATP utilisation has no control in state 4

Table 2
Simulated flux control coefficients for particular enzymes (processes) of oxidative phosphorylation in state 4, state $3_{1/2}$ and state 3

Enzyme (reaction)	State 4	State $3_{1/2}$	State 3
Substrate dehydrogenation	0.04	0.05	0.35
Complex III	0.00	0.00	0.01
Cytochrome oxidase	0.17	0.10	0.15
Proton leak	0.79	0.21	0.02
ATP synthase	0.00	0.00	0.04
ATP/ADP carrier	0.00	0.01	0.28
Phosphate carrier	0.00	0.00	0.05
ATP utilization	0.00	0.63	0.10

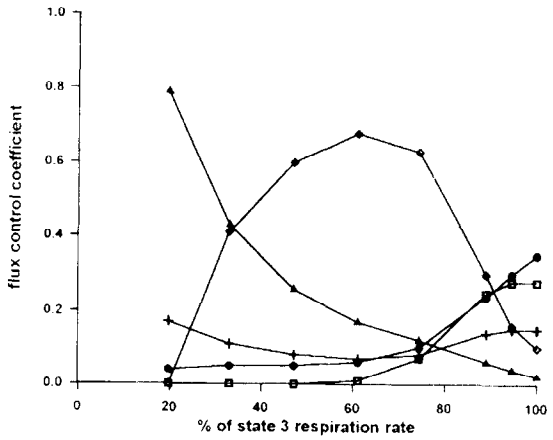

Fig. 1. Simulated flux control coefficients with respect to the oxygen consumption flux for chosen enzymes (processes) of the oxidative phosphorylation system as a function of the respiration rate. (●), substrate dehydrogenation, (+), cytochrome oxidase, (□), ATP/ADP carrier, (◇), ATP utilization, (▲), proton leak.

as there is no phosphorylation flux. It has also almost no control near state 3, as ATP concentration is there below the Michaelis–Menten constant (K_m) of hexokinase to ATP and therefore hexokinase activity is very sensitive to ATP concentration (the elasticity of hexokinase towards ATP concentration is high). In the intermediate states, the ATP utilisation has a high flux control coefficient as there is a significant phosphorylation flux and ATP concentration is far above the K_m constant of hexokinase (and therefore this enzyme is almost insensitive to ATP concentration – the elasticity of hexokinase to [ATP] is low). The flux control coefficient for proton leak is close to 1 in state 4 since this process is the unique consumer of Δp under these conditions and proton leak is much less sensitive to Δp than the cytochrome oxidase and substrate dehydrogenation. Inversely, in state 3 this coefficient is near 0 as Δp is mostly used for ATP synthesis and not dissipated into heat. The control over the respiration flux kept by the cytochrome oxidase does not change significantly between state 4 and state 3. The ATP/ADP carrier and substrate dehydrogenation have almost no control in state 4 and state $3_{1/2}$. However, in state 3 their capacities for the flux intensity become saturated and their flux control coefficients increase very significantly. A similar situation occurs in the case of the ATP synthase and phosphate carrier; however, the

values of flux control coefficients are much smaller here.

Simulated flux control coefficients for the oxidation, phosphorylation and proton leak subsystems with respect to the oxidation flux for different values of the respiration rate are shown in Fig. 2. The theoretical values are very similar to experimental results obtained by Hafner et al. [5] in the frame of the 'top-down' approach to metabolic control analysis. Since flux control coefficients of entire subsystems are sums of flux control coefficients of their components, the pattern of control presented in Fig. 2 results from the patterns in Fig. 1 and Table 2.

The flux control coefficients for the three distinguished subsystems with respect to the phosphorylation flux for state 4, state 3 and the intermediate states are presented in Fig. 3. Again, a very good agreement with experimental results [5,25] can be observed. Both the experimental and theoretical data show that near state 4 and state $3_{1/2}$ the phosphorylation subsystem is mainly controlled by itself (flux control coefficient very near 1), because under these conditions an external ATP concentration is far above the K_m constant of hexokinase and this enzyme is practically insensitive to any intermediate metabolite concentration. Unlike the oxidation flux, the entire phosphorylation flux passes through hexokinase; there is no 'buffering' by proton leak. Therefore hexokinase is able to keep almost all the

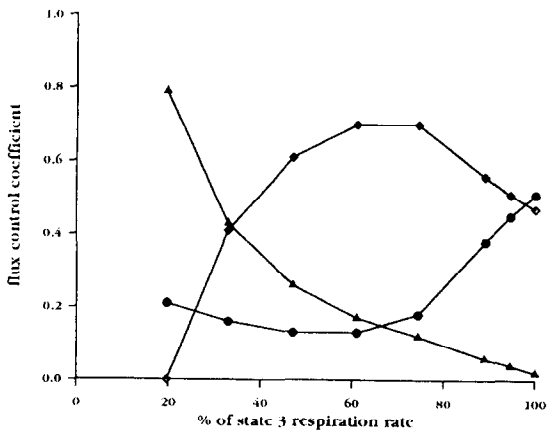

Fig. 2. Simulated flux control coefficients with respect to the oxidation (oxygen consumption) flux for the oxidation, phosphorylation and proton leak subsystems. (●), oxidation subsystem, (◇), phosphorylation subsystem, (▲), proton leak subsystem.

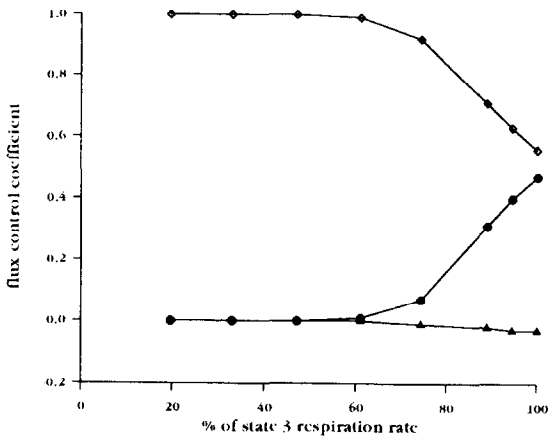

Fig. 3. Simulated flux control coefficients with respect to the phosphorylation flux for the oxidation, phosphorylation and proton leak subsystems. (●), oxidation subsystem, (◇), phosphorylation subsystem, (▲), proton leak subsystem.

control over the phosphorylation flux under the conditions discussed. Near state 4 the concentration of ATP falls below the K_m constant of hexokinase for this compound, the capacity of the oxidation subsystem for flux intensity becomes exhausted resulting in the flux control coefficient for this subsystem equal to about 0.5. The rest of the control under these conditions is kept by the phosphorylation subsystem (ATP/ADP carrier and, additionally, ATP synthase and phosphate carrier; the ATP utilisation near state 4 has a low value of the flux control coefficient). Proton leak exerts no significant control over the phosphorylation flux at all values of the respiration rate.

Finally, Fig. 4 presents simulated flux control coefficients of the three subsystems with respect to the proton leak flux. These values are also consistent with experimental results [5,25]. Proton leak controls the proton leak flux at different values of the respiration rate to a similar extent (flux control coefficient equal to about 0.8). Passing from state 4 to state 3 the oxidation subsystem exerts an increasing positive control and the phosphorylation subsystem an increasing negative control over the proton leak flux. This is connected with a decreasing absolute value of intensity of this flux and increasing absolute intensities of the oxidation and phosphorylation fluxes.

Figs. 5–8 show time courses of chosen parameter values after addition of a small amount of ADP

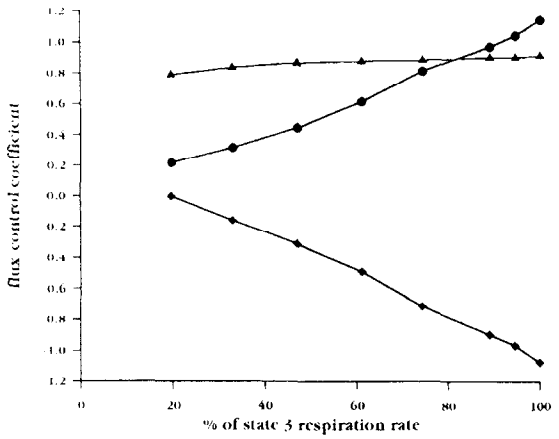

Fig. 4. Simulated flux control coefficients with respect to the proton leak flux for the oxidation, phosphorylation and proton leak subsystems. (●), oxidation subsystem, (◇), phosphorylation subsystem, (▲), proton leak subsystem.

(corresponding to about 200 nmol ADP per mg of mitochondrial protein) to mitochondria in state 4. Mitochondria transfer to state 3 and, after about 2 minutes (when all ADP is converted to ATP), they return to state 4. All the values of the parameters important for regulation of oxidative phosphorylation follow these changes. The respiration rate increases rapidly after the ADP addition (Fig. 5) and subsequently it decreases slowly (there is a quasi-plateau) in time as ADP is being exhausted. When ADP is completely depleted (compare Fig. 8) the respiration rate quickly falls to the state 4 value. The protonmotive force, conversely, decreases after the transition to state 3, then slowly increases (quasi-plateau)

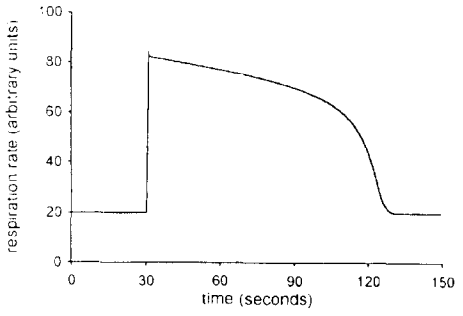

Fig. 5. Time course of the respiration rate after an addition (after 30 s) of a small amount of ADP. The respiration rate is expressed in arbitrary units, which correspond approximately to nmol $O_2 \cdot mg$ protein$^{-1} \cdot min^{-1}$.

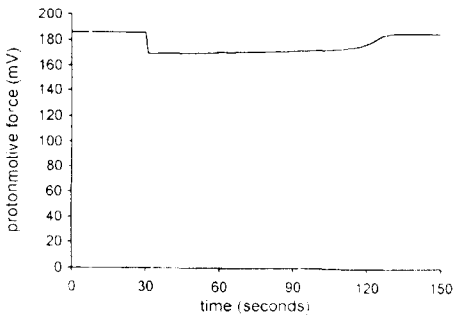

Fig. 6. Time course of the protonmotive force after an addition (after 30 s) of a small amount of ADP.

and during the return to state 4 increases more quickly and reaches its initial value (Fig. 6). These theoretical simulations are consistent, at least semi-quantitatively, with experimental results [28,29]. Both experiments and simulations show that there is no constant value of the respiration rate and Δp in state 3 obtained by an addition of ADP (especially if small amounts of this compound are added). State 3 obtained by an addition of an ADP-regenerating system (e.g. hexokinase + glucose) is more stable and therefore better defined. Furthermore, the increase in the respiration rate and the decrease in Δp is somewhat greater in state 3 induced by the regeneration of ADP from ATP than in state 3 established by the addition of ADP. The reason for this is that adenylate kinase very quickly converts most of the added ADP to ATP and AMP (compare Fig. 8), and the phosphorylation potential is always higher than the phosphorylation potential obtained during continuous consumption of ATP (in the latter case there is, at the same equilibrium constant of the reaction

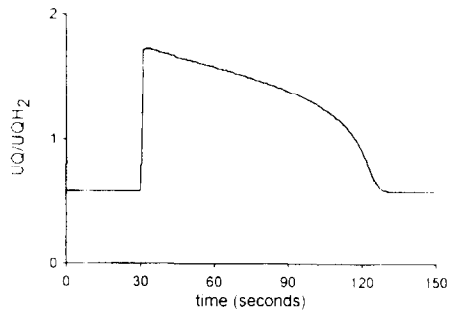

Fig. 7. Time course of the UQ/UOH_2 ratio after an addition (after 30 s) of a small amount of ADP.

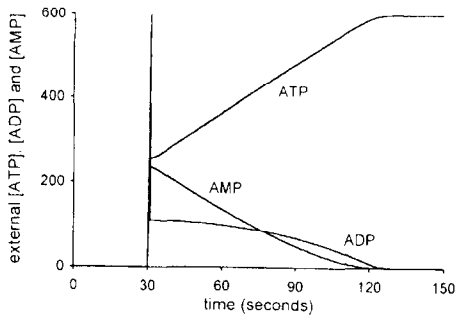

Fig. 8. Time course of external concentration of ATP, ADP and AMP after an addition (after 30 s) of a small amount of ADP.

catalysed by adenylate kinase, relatively more AMP and less ATP, as the latter is very rapidly converted to ADP). Finally, state 3 generated by the addition of the ADP-regenerating system is more physiological, as this system corresponds to the ATP usage in intact cells. It should be emphasised that relatively very small changes in Δp cause great relative changes in the respiration rate. This property reflects the great sensitivity of the oxidation subsystem to the protonmotive force.

Fig. 7 shows changes in time of the UQ/UQH_2 ratio during the simulated experiment. This time course is similar to the time course of the respiration rate. It can be explained by a near-proportional dependence of the substrate dehydrogenation flux intensity on this ratio. Therefore changes in UQ/UQH_2 follow changes in the respiration rate (and reversely).

The majority of ADP added to suspension of mitochondria in state 4 is almost immediately converted by adenylate kinase to ATP and AMP (Fig. 8). The reaction catalysed by this enzyme is very fast, so adenylate kinase works near equilibrium. This can explain very sharp changes immediately after onset of state 3. Afterwards, the remaining ADP is gradually converted to ATP. However, concentration of ADP drops relatively slowly, as it is effectively buffered by changes in [AMP]. This mechanism is responsible (at least partially) for the quasi-plateau in the time course of external ADP concentration, respiration rate, protonmotive force and other parameters in the simulated experiment. Therefore, we can consider adenylate kinase as an enzyme buffering the external phosphorylation potential (compare [30,31]). It must be emphasized that the above considerations concern mitochondria suspended in a medium containing Mg^{2+}. Adenylate kinase needs magnesium-bound forms of ATP and ADP for its activity; without this ion the enzyme is inactive. Therefore the state 4 → state 3 → state 4 transition is not so well expressed in magnesium-free suspensions of mitochondria. In the simulation without an external magnesium ion pool the initial changes in the ATP and ADP concentrations were not so rapid and the plateau in time courses of all parameters much less pronounced. The medium containing Mg^{2+} ions is more physiologically relevant than the magnesium-free medium, because in intact cells there is a considerable concentration of magnesium ions in the cytosol (0.38 mM). This is one of the reasons why the state 3 experiment performed by Ogawa and Lee [13], which was modelled by Holzhütter et al. [14], does not represent a typical state 4 → state 3 transition well. The other reasons are the unusually high concentration of mitochondria in suspension and the low temperature used.

When all the ADP added is converted to ATP (about 2 minutes after the addition), the values of all parameters (except of, of course, the external ATP concentration) return to their initial state 4 values. However, transition from state 3 to state 4 is less sharp here than the onset of state 3. Both state 4 → state 3 and state 3 → state 4 transitions are less clear in a magnesium-free medium.

In the theoretical model of oxidative phosphorylation used in the present paper a H^+/ATP stoichiometry of ATP synthesis by ATP synthase (n_a) equal to 2.5 H^+/ATP was used. Integer values of this parameter equal to 2 or 3 are usually considered in literature [32–39]. What is the motive of such a treatment? Thermodynamic calculations of n_a, based on measurements of Δp and the phosphorylation potential ($ATP/ADP \cdot P_i$) give most frequently values between 2 and 3, gathering roughly around 2.5 [13,26,40]. However, one can argue that the measurement of one (or more) of the parameter values, for example free ADP or Δp, is not very accurate, and that the exact 'true' value would give an integer value of n_a. However, ATP synthase working near equilibrium is not the only thermodynamic requirement which has to be taken into account. The thermodynamic relationships of different reactions create a network, because many of them have common

metabolites. A part of this network, which was taken explicitly into account in the model, is shown in Table 3. This network imposes, for example, a unique Δp value fixed unequivocally by other parameter values and by thermodynamic requirements for particular reactions. It is impossible to change the protonmotive force to the value which would give an integer stoichiometry for ATP synthesis without disturbing seriously the thermodynamic limitations for the ATP/ADP carrier, phosphate carrier and respiratory chain. The same can be said about other parameters. The additional enzyme belonging to the network of thermodynamic dependencies, not shown in Table 3, is adenylate kinase. Thus, the network is sophisticated enough to determine unequivocally the value of n_a. The measured values of all parameters fit very well to each other to fulfil the thermodynamic requirements of particular reactions. Change in one parameter would require strictly determined changes in many other parameters. Therefore we have two possibilities to choose. Either there are great errors in the measured values of many parameters and all these errors are by a chance of a size exactly needed to fulfil the mentioned thermodynamic requirements, or the H^+/ATP stoichiometry for ATP synthesis is not integer and is equal to about 2.5.

In the present paper (and in the accompanying paper) the developed mathematical model of oxidative phosphorylation was successfully tested for isolated mitochondria (and intact cells) in a broad range of conditions. The agreement of the theoretical simulations with experimental results was at least semi-quantitative and in many cases very good. An entirely quantitative comparison is not possible, because experimental results differ somewhat from each other because of different procedures, conditions and sources of mitochondria used. Furthermore, in such a sophisticated system as oxidative phosphorylation there is some inherent variability on the macroscopic level. Small, undetectable changes on the microscopic level can cause relatively significant variations of measured parameters. Therefore the theoretical results produced using the model should be compared with typical experimental values of parameters or their ranges.

The model described in the present paper is only quasi-mechanistic, as described in the accompanying paper. The description of substrate dehydrogenation and, partially, of the ATP/ADP carrier is certainly phenomenological (one of the aims of the model was to find proper descriptions for these components of the system). Therefore, this model should be carefully tested in a broad range of conditions, what was the main purpose of the present paper. Such a tested model, correctly describing many different properties of oxidative phosphorylation, could serve as an useful tool for prediction and explanation of quantitative properties of the system which are intuitively not obvious. The kinetic descriptions of particular enzymes (processes) need not to be entirely 'true' in a mechanistic sense. It is enough, if they are correct in a functional sense, i.e. if they are able to reflect correctly a complex pattern of properties of the studied system.

A phenomenological description has some advantages in relation to a fully mechanistic description. Its validity does not depend on uncertainties in our knowledge about the system. For example, the semi-phenomenological description of the ATP/ADP carrier is not 'sensitive' to the fact whether or not the process of channelling, proposed by some authors for this carrier [41,42], takes place. The model does not distinguish between proton leak [28,43] and pump slipping [44] either, and therefore does not depend on which of them occurs.

A constant H^+/ATP stoichiometry was accepted

Table 3
A network of thermodynamic dependencies within oxidative phosphorylation in isolated mitochondria. The network is balanced only under the assumption that ATP synthase uses about 2.5 protons for synthesis of 1 ATP. Both stoichiometries 2 and 3 H^+/ATP give results far from balance

Enzyme	Parameters involved	Thermodynamic requirement
Phosphate carrier	Δp (ΔpH), P_{ii}, P_{ic}	near equilibrium
ATP/ADP carrier	Δp ($\Delta\Psi$), ATP_i, ADP_i, ATP_c, ADP_c	about 30 times displaced from equilibrium [46]
Respiratory chain	Δp, cyt.c^{3+}/cyt.c^{2+}, UQ/UQH_2	near equilibrium
ATP synthase	Δp, ATP_i, ADP_i, P_{ii}	near equilibrium

in the model discussed. The proposition that this stoichiometry can be regulated [45] needs further confirmation.

Of course the model of the oxidative phosphorylation process described in this paper and in the accompanying paper is not fully completed as it can be further improved and extended. However, it seems to be a broadly tested approximation good enough to describe mechanisms responsible for control and regulation of this process in mammalian mitochondria (especially rat liver mitochondria) semiquantitatively, to calculate the parameter values which biochemists are interested in, and to derive macroscopic properties of the entire system from microscopic features of its components. Therefore it can be used to try to predict the results of new kinds of experiments, not performed until now, and to explain some experimental properties which are not obvious intuitively.

Acknowledgements

This work was supported by Komitet Badań Naukowych.

References

[1] B. Chance and G.R. Williams, Adv. Enzymol.,17 (1956) 65–134.
[2] M.D. Brand and M.P. Murphy, Biol. Rev., 62 (1987) 141–193.
[3] G.C. Brown, Biochem. J., 284 (1992) 1–13.
[4] J.E. Hassinen, Biochim. Biophys. Acta, 853 (1986) 135–151.
[5] R.P. Hafner, G.C. Brown and M.D. Brand, Eur. J. Biochem., 188 (1990) 313–319.
[6] K.F. LaNoue, J. Bryla and J.R. Williamson, J. Biol. Chem., 247 (1972) 667–679.
[7] F.N. Gellerich, R. Bohnensack and W. Kunz, Biochim. Biophys. Acta, 722 (1983) 381–391.
[8] A.K. Groen, R.J.K. Wanders, H.V. Westerhoff, R. van der Meer and J.M. Tager, J. Biol. Chem., 257 (1982) 2754–2757.
[9] J.M. Tager, R.J.A. Wanders, A.K. Groen, W. Kunz, R. Bohnensack, U. Koster, G. Letko, G. Bohme, J. Duszyński and L. Wojtczak, FEBS Lett., 151 (1983) 1–9.
[10] M. Erecińska, R.L. Veech and D.F. Wilson, Arch. Biochem. Biophys., 160 (1974) 412–421.
[11] R. Bohnensack, F.N. Gellerich, L. Schild and W. Kunz, Biochim. Biophys. Acta, 1018 (1990) 182–184.
[12] J. Duszyński, K. Bogucka and L. Wojtczak, Biochim. Biophys. Acta, 767 (1984) 540–547.
[13] S. Ogawa and T.M. Lee, J. Biol. Chem., 259 (1984) 10004–10011.
[14] H. Kacser and J. Burns, Symp. Soc. Exp. Biol., 27 (1973) 65–107.
[15] R. Heinrich and T.A. Rapoport, Eur. J. Biochem., 42 (1974) 107–120.
[16] H. Kacser and J.W. Porteous, Trends Biochem. Sci., 12 (1987) 5–14.
[17] H. Rottenberg, Biochim. Biophys. Acta, 549 (1979) 225–253.
[18] H.V. Westerhoff and K. van Dam, Thermodynamics and Control of Biological Free-Energy Transduction, Elsevier, Amsterdam, 1987.
[19] B.H. Groen, J.A. Berden and K. van Dam, Biochim. Biophys. Acta, 1019 (1990) 121–127.
[20] H.-G. Holzhütter, W. Henke, W. Dubiel and G. Gerber, Biochim. Biophys. Acta, 810 (1985) 252–268.
[21] R. Bohnensack, Biochim. Biophys. Acta, 634 (1981) 203 218.
[22] R. Bohnensack, U. Küster and G. Letko, Biochim. Biophys. Acta, 680 (1982) 271–280.
[23] B. Korzeniewski and W. Froncisz, Biochim. Biophys. Acta, 1060 (1991) 210–223.
[24] B. Korzeniewski and W. Froncisz, Biochim. Biophys. Acta, 1102 (1992) 67–75.
[25] M.D. Brand, in P.W. Hochachka, P.L. Lutz, T. Sick, M. Rosenthal and G. van den Thillart (Editors), Surviving Hypoxia, CRC Press, Boca Raton, 1993, pp. 295–309.
[26] C.A.M. Marres and S. de Vries, Biochim. Biophys. Acta, 1057 (1991) 51–63.
[27] J.G. Reich and E.E. Sel'kov, in Metabolism of the Cell, A Theoretical Treatise, Academic Press, London, 1982.
[28] D.G. Nicholls, Eur. J. Biochem., 50 (1974) 305–315.
[29] D.G. Nicholls and S.J. Ferguson, in Bioenergetics 2, Academic Press, London, 1992.
[30] J.W. Stucki, Eur. J. Biochem., 109 (1980) 269–283.
[31] J.W. Stucki, Eur. J. Biochem., 109 (1980) 257–267.
[32] J. Duszyński, K. Bogucka, G. Letko, U. Küster and L. Wojtczak, in E. Quagliariello, F. Palmieri, S. Papa and M. Klingenberg (Editors), Function and Molecular Aspects of Biomembrane Transport, Elsevier, Amsterdam, 1979, pp. 309–312.
[33] A.L. Lehninger and B. Reynafarje, in K. van Dam and B.F. Gelder (Editors), Structure and Function of Energy-Transducing Membranes, Elsevier, Amsterdam, 1979, pp. 95–106.
[34] M.D. Brand and A.L. Lehninger, Proc. Natl. Acad. Sci. USA, 74 (1977) 1955–1959.
[35] A. Alexandre, B. Reynafarje and A.L. Lehninger, Proc. Natl. Acad. Sci. USA, 75 (1978) 5296–5300.
[36] M.D. Brand, W.G. Harper, D.G. Nicholls and W.J. Ingledew, FEBS Lett., 95 (1978) 125–129.
[37] P.C. Hinkle and M.L. Yu, J. Biol. Chem., 254 (1979) 2450–2455.
[38] P.C. Hinkle, in V.P. Skulachev and P.C. Hinkle (Editors), Chemiosmotic Proton Circuits in Biological Membranes, Addison-Wesley Publishing Co., Reading, MA, 1981, pp. 49–58.
[39] J.J. Lemasters and W.H. Billica, J. Biol. Chem., 256 (1981) 12949–12957.

[40] D.G. Nicholls and V.S.M. Bemson, Eur. J. Biochem., 75 (1977) 601–612.
[41] F.N. Gellerich, FEBS Lett., 297 (1992) 55–58.
[42] F.N. Gellerich and V.A. Saks, Biochem. Biophys. Res. Commun., 105 (1982) 1473–1481.
[43] M.D. Brand, L.-F. Chien and P. Diolez, Biochem. J., 297 (1994) 27–29.
[44] D. Pietrobon, G.F. Azzone and D. Walz, Eur. J. Biochem., 117 (1981) 389–394.
[45] M. Rigoulet, L. Fraisse, R. Ouhabi, B. Guerin, E. Fontaine and X. Leverve, Biochim. Biophys. Acta, 1018 (1990) 91–97.
[46] M. Klingenberg, in A.N. Martinosi (Editor), The Enzymes of Biological Membranes, Vol. 4, Plenum Press, New York, 1985.